Band-rejection filter based on a Bragg fiber with a defect layer

Zhongjiao He (何忠蛟)

College of Information and Electronic Engineering, Zhejiang Gongshang University, Hangzhou 310035, China

E-mail: he335577@163.com

Received May 8, 2009

A novel band-rejection filter based on a Bragg fiber with a defect layer is proposed. A defect layer is introduced in the periodic high/low index layers in the cladding of the Bragg fiber, which results in large confinement loss for some resonant wavelengths inside the band gap range of the Bragg fiber. A segment of the Bragg fiber with a defect layer can be used as a band-rejection filter, whose characteristics are mainly determined by the structure of the Bragg fiber. The simulation results show that the bandwidth of such a band-rejection filter is dependent on the number of the periodic high/low index layers in both sides of the defect layer in the cladding of the Bragg fiber.

OCIS codes: 060.2310, 060.2280, 120.2440.

doi: 10.3788/COL20100803.0259.

Bragg fibers[1−6] as one kind of photonic crystal fibers (PCFs)[1−15] have attracted considerable attention over the past decade because of their interesting dispersion and modal properties and advances in fabrication techniques. The principle of one-dimensional (1D) photonic band gap ensures that a segment of Bragg fiber can be used as a tunable band-pass filter with a bandwidth up to the order of hundreds of nanometers[16]. With modulated refractive index distributed in transmission direction of the fiber, fiber Bragg grating (FBG)[17] and long period grating (LPG)[18], as two of the most important and well-known fiber filters, have been well developed due to their advantages including compactness and fiber compatibility. However, for most FBGs and LPGs, a complex and costly fabrication system is usually needed, although some low-cost methods have also been proposed.

In this letter, a novel band-rejection filter based on a Bragg fiber with a defect layer is proposed. By employing a defect layer in the cladding of the Bragg fiber, relatively large loss of the transmissive light of some specific wavelengths appears inside the band gap of Bragg fiber, which results in a band-rejection filter with the similar transmision characteristics and similar operation principle as the LPG has. Although a defect Bragg fiber has been reported for broadband and zero dispersion slow light[19], its application as a band-rejection filter has not been investigated.

The cross section and refractive index profile of the proposed Bragg fiber with a defect layer are shown in Fig. 1. A hollow core with a refractive index of 1 and a radius of $r = 2.5$ μm is surrounded by a multilayer cladding which consists of 7 alternating layers of high and low refractive indices. The high (low) refractive index layers are shown in black (gray). We choose high (low) refractive index of 4.6 (1.6) (the same as what has been used in several previous publications[1,2]) with thicknesses of $d_1 = 0.2176\Lambda$ and $d_2 = 0.7824\Lambda$, where the thickness of the periodic two-layer structure is $\Lambda = d_1 + d_2 = 0.3875$ μm. Among the 7 periodic high/low refractive index layers in the radial direction of the Bragg fiber, a defect layer with a refractive index n_1 and a thickness $d_0 = 2d_1$ is introduced in the fourth periodic high/low refractive index layers.

It is well known that the light is confined by the 1D photonic band gap of the multilayer cladding, which is easy to analyze in the limit as the cladding becomes planar. Figure 2 shows the 1D band gaps of the planar dielectric mirror which consists of alternating layers of high/low (4.6/1.6) refractive indices. The surface-parallel wave-vector component β and the frequency

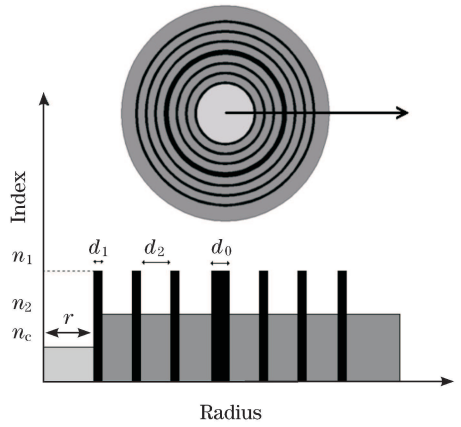

Fig. 1. Cross section and refractive index profile of the Bragg fiber with a defect layer.

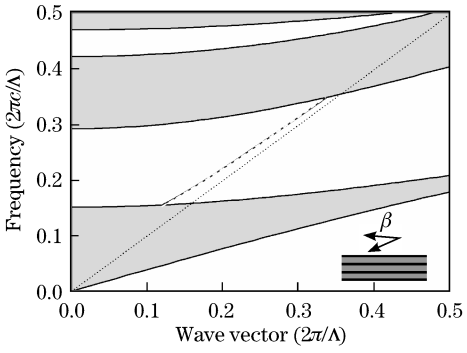

Fig. 2. Band structure of the planar dielectric mirror and dispersion property for TE_{01} mode of the Bragg fiber with a defect layer.

ω are with the unit of $2\pi c/\Lambda$ and $2\pi/\Lambda$, respectively. The gray regions represent the situations where light can propagate in the planar dielectric mirror. The white regions show the band gap of the planar dielectric mirror. The dotted line represents the light line ($\omega = c\beta$). Note that we only consider the TE mode band gap and the low loss TE_{01} mode of the Bragg fiber for the ease of discussion. A full-vector finite-element method[20] can achieve reliable simulation results, as given in some previous papers[11,12] as well as our recent work[21,22]. In this letter, it is employed to achieve the effective modal index and the confinement loss of the Bragg fiber. The dashed line in Fig. 2 shows the dispersion characteristics of TE_{01} mode for the Bragg fiber with 7 periodic high/low refractive index layers and a defect layer in the fourth periodic high/low refractive index layers in the cladding. Calculated results show that the dispersion line of the Bragg fiber with a defect layer almost remains unchanged when the thickness of the defect layer is set to $d_0 = d_1$, corresponding to a conventional Bragg fiber without a defect layer. However, the Bragg fiber with a defect layer shows different characteristics of the confinement loss, which ensures that a Bragg fiber with a defect layer can be used as a band-rejection filter.

Figure 3 shows the confinement loss as a function of wavelength for the Bragg fiber of 7 periodic high/low refractive index layers without a defect layer, the Bragg fiber of 7 periodic high/low refractive index layers with a defect layer, and the Bragg fiber of 9 periodic high/low refractive index layers with a defect layer in the fifth periodic high/low refractive index layers. Note that the confinement loss can be deduced from the imaginary part of the effective modal index[12]. Considering the symmetry of the cross section of the Bragg fiber, we choose one eighth-plane of the Bragg fiber's cross section for calculation. When a defect layer is introduced in the fourth periodic high/low refractive index layers, a confinement loss peak appears around 1530.7 nm inside the band gap region of the Bragg fiber, which is dominated by the parameters of the defect layer. The confinement loss of the Bragg fiber with a defect layer can be effectively reduced by adding more periodic high/low refractive index layers in the cladding. To fully understand the confinement loss peak of the Bragg fiber with a defect layer, we show the normalized intensity distribution of the power flow

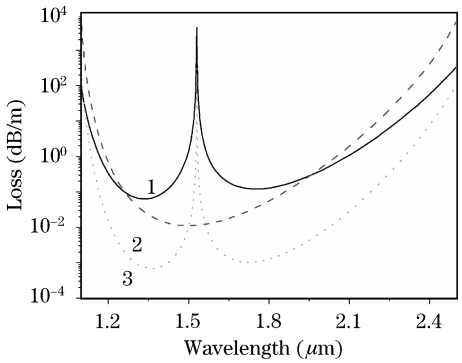

Fig. 3. Confinement of different Bragg fibers. 1: Bragg fiber of 7 periodic high/low refractive index layers with a defect layer; 2: Bragg fiber of 7 periodic high/low refractive index layers without a defect layer; 3: Bragg fiber of 9 periodic high/low refractive index layers with a defect layer.

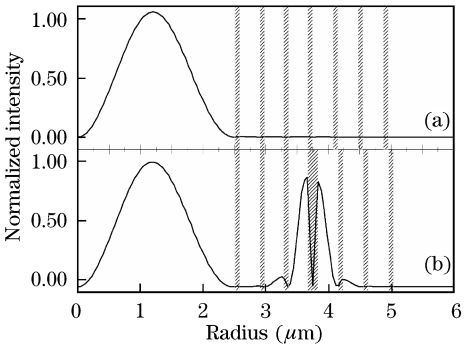

Fig. 4. Normalized intensity distribution of the power flow in the cross section of the Bragg fiber with a defect layer for the wavelength of (a) 1550 and (b) 1530.7 nm.

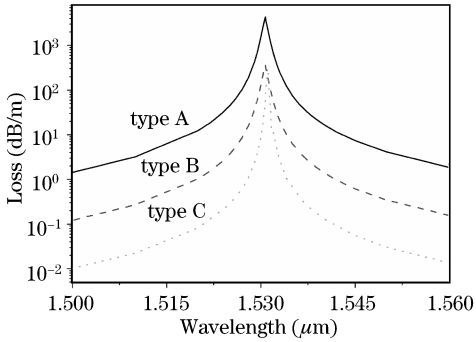

Fig. 5. Confinement loss curves of the three types of the Bragg fibers.

in the cross section of the Bragg fiber with a defect layer for 1550 and 1530.7 nm in Fig. 4. When the wavelength is 1550 nm which is far from the confinement loss peak, light is well confined in the fiber core, which results in a low confinement loss. However, for the light around the confinement loss peak wavelength (1530.7 nm), part of energy with a relatively large fraction of the TE_{01} mode is located in the defect layer, which results in relatively large confinement loss.

The characteristics of the confinement loss of the Bragg fiber with a defect layer indicate that such a Bragg fiber with a suitable length can be used as a band-rejection filter. Figure 5 shows the confinement loss of three types of Bragg fibers. Type A is the Bragg fiber of 7 periodic high/low refractive index layers with a defect layer in the fourth high/low refractive index layers; type B is the Bragg fiber of 8 periodic high/low refractive index layers with a defect layer in the fourth high/low refractive index layers; type C is the Bragg fiber of 9 periodic high/low refractive index layers with a defect layer in the fifth high/low refractive index layers. Figure 6 shows transmission spectra of the band-rejection filters based on a 1.16-cm type A Bragg fiber, a 16.25-cm type B Bragg fiber, and a 13.89-cm type C Bragg fiber. Note that all lengths of the three types of Bragg fibers are set to achieve the normalized 50-dB maximum loss of each band-rejection filter and show the bandwidth comparison of the band-rejection filters based on the three types Bragg fibers. The 25-dB bandwidths of the filters based on type A and type B Bragg fibers are about 1 nm and that of the filter based on type C Bragg fiber is about 0.4 nm, indicating that we can design filters with

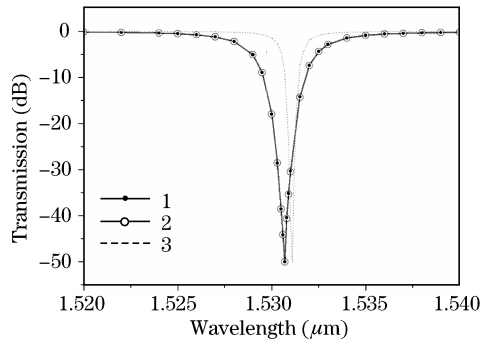

Fig. 6. Transmission spectra of the band-rejection filters based on the three types of Bragg fibers. 1: 1.16 cm, type A; 2: 16.25 cm, type B; 3: 13.89 cm, type C.

different bandwidths by introducing different high/low refractive index layers in the fiber cladding. We have also noted that there is a small difference between the central wavelengths of the filters based on type A (B) Bragg fiber and type C Bragg fiber. It is probably because of the different curvatures of the defect layer in the fourth and fifth high/low refractive index layers, which results in the different effective thicknesses of the defect layers when considering the dielectric mirror of the high/low refractive index layers.

In conclusion, band-rejection filters based on the Bragg fiber with a defect layer have been investigated by employing a full-vector finite-element method. The characteristics of the band-rejection filters based on the Bragg fibers with different structures are investigated. The bandwidth of the proposed band-rejection filter becomes narrower when the number of the high/low refractive index layers in both sides of the defect layer increases, indicating that the bandwidth of the band-rejection filter can be well designed for some specific applications. In addition, according to the theory of the dielectric mirror which consists of alternating layers of high/low refractive indices, we believe that the central wavelength of the proposed filter can be adjusted by changing the index or thickness of the defect layer. The proposed band-rejection filters will have advantages of fabrication consistency and possible applications for strain sensing in the radial direction of the Bragg fiber.

This work was supported by the Foundation of Zhejiang Provincial Education Department under Grant No. Y200803144.

References

1. M. Ibanescu, Y. Fink, S. Fan, E. L. Thomas, and J. D. Joannopoulos, Science **289,** 415 (2000).
2. S. G. Johnson, M. Ibanescu, M. Skorobogatiy, O. Weisberg, T. D. Engeness, M. Soljačić, S. A. Jacobs, J. D. Joannopoulos, and Y. Fink, Opt. Express **9,** 748 (2001).
3. A. Argyros, Opt. Express **10,** 1411 (2002).
4. G. Vienne, Y. Xu, C. Jakobsen, H.-J. Deyerl, J. B. Jensen, T. Sørensen, T. P. Hansen, Y. Huang, M. Terrel, R. K. Lee, N. A. Mortensen, J. Broeng, H. Simonsen, A. Bjarklev, and A. Yariv, Opt. Express **12,** 3500 (2004).
5. T. Katagiri, Y. Matsuura, and M. Miyagi, J. Lightwave Technol. **24,** 4314 (2006).
6. K. J. Rowland, S. Afshar V., and T. M. Monro, J. Lightwave Technol. **26,** 43 (2008).
7. C. M. Smith, N. Venkataraman, M. T. Gallagher, D. Müller, J. A. West, N. F. Borrelli, D. C. Allan, and K. W. Koch, Nature **424,** 657 (2003).
8. J. C. Knight, Nature **424,** 847 (2003).
9. J. C. Knight, J. Broeng, T. A. Birks, and P. St. J. Russell, Science **282,** 1476 (1998).
10. P. Russell, Science **299,** 358 (2003).
11. T. P. Hansen, J. Broeng, S. E. B. Libori, E. Knudsen, A. Bjarklev, J. R. Jensen, and H. Simonsen, IEEE Photon. Technol. Lett. **13,** 588 (2001).
12. D. Chen and L. Shen, IEEE Photon. Technol. Lett. **19,** 185 (2007).
13. A. Argyros, M. A. van Eijkelenborg, M. C. J. Large, and I. M. Bassett, Opt. Lett. **31,** 172 (2006).
14. M. Wu, D. Huang, H. Liu, and W. Tong, Chin. Opt. Lett. **6,** 22 (2008).
15. T. Sun, G. Kai, Z. Wang, S. Yuan, and X. Dong, Chin. Opt. Lett. **6,** 93 (2008).
16. B.-W. Liu, M.-L. Hu, X.-H. Fang, Y.-F. Li, L. Chai, J.-Y. Li, W. Chen, and C.-Y. Wang, IEEE Photon. Technol. Lett. **20,** 581 (2008).
17. K. O. Hill and G. Meltz, J. Lightwave Technol. **15,** 1263 (1997).
18. A. M. Vengsarkar, P. J. Lemaire, J. B. Judkins, V. Bhatia, T. Erdogan, and J. E. Sipe, J. Lightwave Technol. **14,** 58 (1996).
19. C. Lin, W. Zhang, Y. Huang, and J. Peng, J. Lightwave Technol. **25,** 3776 (2007).
20. K. Saitoh and M. Koshiba, IEEE J. Quantum Electron. **38,** 927 (2002).
21. Z. J. He, Acta Photon. Sin. (in Chinese) **36,** 1215 (2007).
22. Z. J. He, Acta Photon. Sin. (in Chinese) **37,** 301 (2008).